

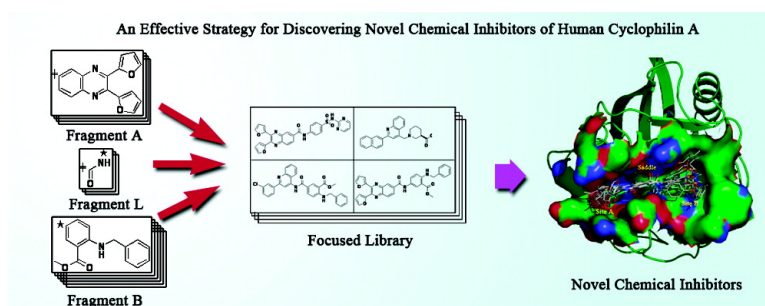
Article

Strategy for Discovering Chemical Inhibitors of Human Cyclophilin A: Focused Library Design, Virtual Screening, Chemical Synthesis and Bioassay

Jian Li, Jian Zhang, Jing Chen, Xiaomin Luo, Weiliang Zhu,
 Jianhua Shen, Hong Liu, Xu Shen, and Hualiang Jiang

J. Comb. Chem., **2006**, 8 (3), 326-337 • DOI: 10.1021/cc0501561 • Publication Date (Web): 13 April 2006

Downloaded from <http://pubs.acs.org> on March 22, 2009



More About This Article

Additional resources and features associated with this article are available within the HTML version:

- Supporting Information
- Links to the 4 articles that cite this article, as of the time of this article download
- Access to high resolution figures
- Links to articles and content related to this article
- Copyright permission to reproduce figures and/or text from this article

[View the Full Text HTML](#)

Strategy for Discovering Chemical Inhibitors of Human Cyclophilin A: Focused Library Design, Virtual Screening, Chemical Synthesis and Bioassay

Jian Li,[†] Jian Zhang,[†] Jing Chen,[†] Xiaomin Luo,[†] Weiliang Zhu,[†] Jianhua Shen,[†]
Hong Liu,^{*,†} Xu Shen,^{*,†,‡} and Hualiang Jiang^{*,†,‡}

Drug Discovery and Design Center, State Key Laboratory of Drug Research, Shanghai Institute of Materia Medica, Shanghai Institutes for Biological Sciences, Graduate School of the Chinese Academy of Sciences, Chinese Academy of Sciences, Shanghai 201203, P. R. China, and School of Pharmacy, East China University of Science and Technology, Shanghai 200237, China

Received December 5, 2005

The discovery of cyclophilin A (CypA) inhibitor is now of special interest in the treatment of immunological disorders. In this work, using a strategy integrating focused combinatorial library design, virtual screening, chemical synthesis, and bioassay, a series of novel small molecular CypA inhibitors have been discovered. First, using the fragments taken from our previously discovered CypA inhibitors (*Bioorg. Med. Chem.* 2006, 14, 2209–2224) as building blocks, we designed a focused combinatorial library containing 255 molecules employing the LD1.0 program (*J. Comb. Chem.* 2005, 7, 398–406) developed by us. Sixteen compounds (**1a–e**, **2a–b**, **3a–b**, and **4a–g**) were selected by using virtual screening against the X-ray crystal structure of CypA as well as druglike analysis for further synthesis and bioassay. All these sixteen molecules are CypA binders with binding affinities (K_D values) ranging from 0.076 to 41.0 μM , and five of them (**4a**, **4c**, and **4e–g**) are potent CypA inhibitors with PPIase inhibitory activities (IC_{50} values) of 0.25–6.43 μM . The hit rates for binders and inhibitors are as high as 100% and 31.25%, respectively. Remarkably, both the binding affinity and inhibitory activity of the most potent compound increase ~ 10 times than that of the most active compound discovered previously. The high hit rate and the high potency of the new CypA inhibitors demonstrated the efficiency of the strategy for focused library design and screening. In addition, the novel chemical entities reported in this study could be leads for discovering new therapies against the CypA pathway.

Introduction

Human cyclophilin A (hCypA), which has been widely studied for mapping its biological functions,¹ is the most important member of the 15 known human cyclophilins. In addition to binding the target of cyclosporin A (CsA), an immunosuppressive drug used to prevent allograft rejection,² CypA plays a critical role in a variety of biological processes, including enhancing the rate of folding/unfolding of proteins via its peptidyl-prolyl isomerase (PPIase) activity,^{3,4} and binding to the HIV-1 Gag polyprotein for facilitating viral replication.⁵ Recently, it was discovered that the nucleocapsid (N) protein of SARS coronavirus (SARS-CoV) can bind to CypA, which may be associated with SARS-CoV infection.^{6,7}

CypA inhibitors are of therapeutic significance in organ transplantation.^{8,9} However, inhibitors of CypA are mainly derived from the nature sources (such as CsA,² FK506,¹⁰ rapamycin¹¹ and sanglifehrin A¹²) and peptide analogues,¹³

which are all structurally complex molecules, and little has been reported regarding the small molecule CypA inhibitors. Recently, based on the hits discovered using virtual screening and bioassay, we have designed and synthesized a series of sulfanilamide and 4,4'-methylenebisanthranilic acid derivatives. Binding assay indicated that most derivatives showed high affinities to CypA and four of them showed PPIase inhibition activities with IC_{50} values at micromolar level.¹⁴

The advent of focused library and virtual screening has reduced the disadvantage of combinatorial chemistry and changed it to a realizable and cost-effective tool in drug discovery.¹⁵ A focused library is built on the basis of a lead molecule or pharmacophore and geared toward one particular molecular target. Extracting fragments from known drugs or ligands (inhibitors or activators) of the studied target is an effective approach for collecting new building blocks. Druglikeness and structural diversity have been introduced into the library design to reduce its size and increase its efficiency. To establish a new efficient approach that can be used to build, optimize and assess focused libraries based on the 3D structures of target receptor, we developed a software package named LD1.0.¹⁵ LD1.0 combines the scores of structural diversity and binding affinity with our newly improved druglikeness scoring functions.¹⁶

* Corresponding author address: Shanghai Institute of Materia Medica, Chinese Academy of Sciences, 555 Zuchongzhi Road, Zhangjiang Hi-Tech Park, Shanghai 201203, China. Phone: +86-21-50806600, ext. 1210. Fax: +86-21-50807088. E-mail: hljiang@mail.shnc.ac.cn (H.J.); hliu@mail.shnc.ac.cn (H.L.); xshen@mail.shnc.ac.cn (X.S.).

[†] Chinese Academy of Sciences.

[‡] East China University of Science and Technology.

In the present paper, we report on the discovery of potent CypA inhibitors by using our new approach of focused library design and screening. First, a focused library consisting of 255 molecules was constructed by using LD1.0.¹⁵ Fragments derived from our previously reported CypA inhibitors¹⁴ were used as the building blocks for the focused library generation. By using docking-based virtual screening targeting the binding pocket of CypA, 16 compounds (**1a–e**, **2a–b**, **3a–b**, and **4a–g**) were selected for synthesis and bioassay. All of these 16 compounds showed higher binding affinities to CypA, with K_D values of 0.076–41.0 μM , and 5 of them (compounds **4a**, **4c**, and **4e–g**) show high CypA PPIase inhibition activities, with IC_{50} values of 0.25–6.43 μM . Both the binding affinity and inhibitory activity of the most potent compound increase ~ 10 times over that of the most active compound discovered previously.¹⁴ The effectiveness of our approach for focused library design and screening was demonstrated by the high hit rate and high potency of the CypA inhibitors. In addition, the novel active chemical entities reported here should be good leads for discovering new therapies against the CypA pathway.

Materials and Methods

Focused Combinatorial Library Design and Virtual Screening. 1. Library Design. In our previous study,¹⁴ we discovered dozens of binders of CypA with binding affinities under submicromolar or micromolar levels, and 14 of them showed high CypA PPIase inhibition activities, with IC_{50} 's of 2.5–6.2 μM . To discover new chemical entities of CypA inhibitors with more potent activities, a focused library was designed on the basis of the structures of the 14 inhibitors and their modes of binding to CypA. The LD1.0 program¹⁵ was used in the focused library designing. LD1.0 is a software developed in our laboratory for designing a combinatorial library. It encoded a new approach for generating a target-focused library using the combination of the scores of structural diversity and binding affinity with our newly improved druglikeness scoring functions.¹⁶

According to the binding models of previously discovered inhibitors to CypA,^{14,17} the small-molecular CypA inhibitors can be divided into three parts: part A interacts with the small pocket of CypA (site A), part B is located in the large pocket (site B), and part L is a linker between A and B, interacting with the "saddle" pocket between sites A and B. From the CypA binders (or inhibitors) discovered previously¹⁴ and their modes of interaction with CypA, we selected 5 fragments for part A, 17 fragments for part B, and 3 linkers for part L. The chemical structures of the fragments are shown in Figure 1. These fragments from different parts could react with each other to generate 255 molecules. Starting from these fragments and on the basis of the X-ray crystal structure of CypA (PDB entry 1NMK),¹² the software LD1.0 was employed to build a CypA-focused library with a population of $5 \times 3 \times 17$. Default parameters in LD1.0¹⁵ were used for constructing the focused library.

2. Library Virtual Screening. The binding potential between CypA and molecules in the combinatorial library was evaluated by the scoring module of LD1.0. Docking

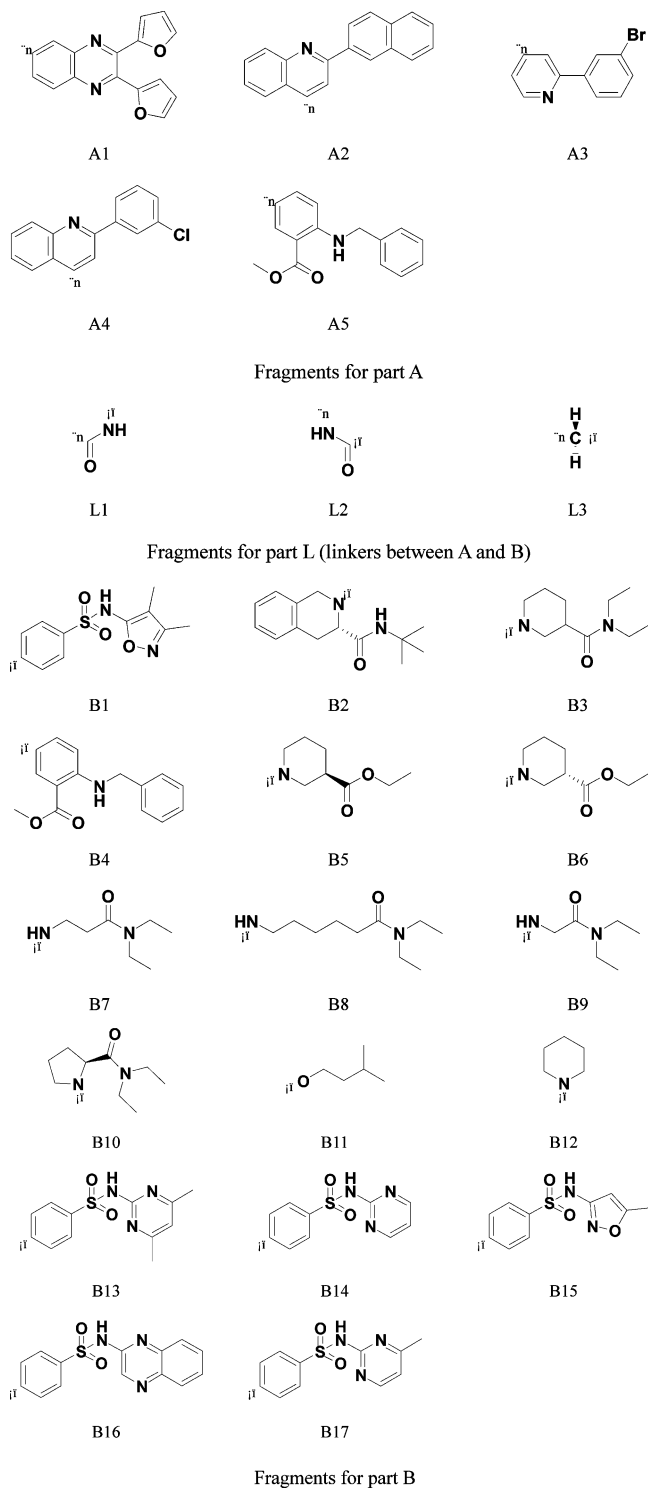


Figure 1. Building blocks for focused library generation. Fragments for parts A, B, and L were isolated for our previously discovered CypA binders and inhibitors.^{14,17} The symbols + and ★ represent the sites where fragments connect each other to form a complete structure.

algorithms and scoring functions of DOCK4.0^{18,19} and AutoDock3.05²⁰ were adopted by the scoring module of LD1.0. Thus, we used two scoring systems to avoid the inaccuracy of one scoring function. The X-ray crystal structure of CypA¹² was used as a target for the virtual screening. Residues of CypA around the binding site at a radius of 6.5 Å were isolated for constructing the grids of the docking screening. The resulting substructure included

all residues of the binding pocket. During the docking simulation, Kollman-all-atom charges²¹ were assigned to the protein, and Gasteiger–Marsili charges²² were assigned to the molecules in the library. Conformational flexibility of the molecules from the library was considered in the docking search.

3. Druglike Analysis. The druglikeness of molecules from the combinatorial library was also evaluated by the druglikeness module of LD1.0.¹⁵ The druglikeness descriptor set encoded in LD1.0 is composed of the “Rule of Five” and the other three descriptors of structural ratio.^{16,23} For obtaining more information and demand of synthetical alternation, we broadened the constraint of molecular weight to 600. The range of evaluation on druglikeness is between 0 and 1, which stand for nondruglikeness and druglikeness, respectively.¹⁶ All the parameters used in the LD1.0 were described in our previous paper.¹⁵

Chemical Synthesis. On the basis of evaluation of binding potential and druglikeness, we selected 16 compounds (**1a–e**, **2a,b**, **3a,b**, and **4a–g**) (Table 1) for synthesis and bioassay.

Scheme 1 depicts the sequence of reactions that led to the preparation of compounds **1a–e** using isatin **5** as the starting material. In general, the substituted 4-quinolinecarboxylic acids **6** were prepared by isatin **5** condensation with ketones in ethanol.²⁴ The carboxyl group in **6** was successfully converted to chloride **9** by a sequential esterification, reduction, and chlorination. Replacement of the resulting chloride by reacting with amines under reflux conditions in NMP gave the targeted compounds **1a–e**.

Compounds **2a,b** were synthesized through the route outlined in Scheme 2. Compound **7** was reacted by refluxing with 85% hydrazine monohydrate in C₂H₅OH, which afforded quinoline-4-hydrazide (**10**). Compound **10** was transformed to the key intermediate **12** by employing diazotization and Curtius reactions.²⁵ Reaction of **12** with isoamyl alcohol and (*R*)-(–)-ethyl nipecotate²⁶ in refluxing toluene afforded compounds **2a** and **b**, respectively.

Scheme 3 depicts the sequence of reactions that led to the preparation of compounds **3a,b** using 1,3-dimethyl-4-nitrobenzene, **14**, as the starting material. Compound **15**²⁷ was synthesized by KMnO₄-promoted oxidation of methyl groups in **14**, followed by esterification and selective hydrolysis, a procedure developed by Axer.²⁸ After chlorination of acid and N-acylation, compound **19** was obtained, and then **19** was reduced by Sn in the mixture of hydrochloric acid and ethanol to give **20**. Finally, reaction of compound **20** with benzyl bromide in refluxing NMP afforded compounds **3a,b**.

Compounds **4a–g** were synthesized through the route outlined in Scheme 4. Condensation of the furil **25** with 3,4-diaminobenzoic acid **26** gave adduct **27**. Compound **27** was converted to the corresponding acyl chlorides by reacting with SOCl₂, which was then substituted by using different sulfanilamides and **24** to provide the targeted compounds **4a–g**. The key intermediate **24** of compound **4a** was prepared from compound **21** by esterification, N-benzylation, and reduction.²⁹

Biological Assay. 1. Binding Affinity Determination. CypA was expressed and purified according to our previously reported procedure.⁶ The binding affinities of compounds

1–4 to CypA *in vitro* were determined by employing surface plasmon resonance (SPR) technology. The measurement was performed using the dual flow cell Biacore 3000 instrument (Biacore AB, Uppsala, Sweden). Immobilization of the CypA to the hydrophilic carboxymethylated dextran matrix of the sensor chip CM5 (Biacore) was carried out by the standard primary amine coupling reaction wizard. The CypA covalently bound to the matrix was diluted in 10 mM sodium acetate buffer (pH 6.0) to a final concentration of 0.035 mg/mL. Equilibration of the baseline was completed by a continuous flow of HBS-EP running buffer (10 mM Hepes, 150 mM NaCl, 3 mM EDTA, and 0.005% (v/v) surfactant P20, pH 7.4) through the chip for 1–2 h. All the Biacore data were collected at 25 °C with HBS-EP as running buffer at a constant flow of 30 μL/min. All the sensorgrams were processed by using automatic correction for nonspecific bulk refractive index effects. The equilibrium constants (*K*_D values) evaluating the protein–ligand binding affinities were determined by the steady-state affinity fitting analysis of the Biacore data.

2. Enzymatic Activity Assay. CypA PPIase activity was measured at 4 °C by using the standard chymotrypsin-coupled assay.³⁰ The assay buffer (50 mM Hepes, 100 mM NaCl, pH 8.0) and CypA (500 nM stock solution) were precooled to 4 °C, to which then was added 15 μL of 3 mg/mL chymotrypsin in 1 mM HCl. The reaction was initiated by adding 12 μL of 3.8 mM peptide substrate (Suc-Ala-Ala-*cis*-Pro-Phe-*p*NA) in LiCl/THF solution with rapid inversion. After a delay from the onset of mixing (usually 6 s), the absorbance of *p*-nitroaniline was followed at 390 nm until the reaction was complete (1 min). The final concentration of LiCl in the assay was 9.6 mM; THF was present at a concentration of 2% (v/v). Absorbance readings were collected every 0.1 s by a U-2010 spectrophotometer. The progress curves were analyzed by nonlinear least-squares fit.

The inhibition assays of compounds were performed in the same manner as the above-mentioned. A 0.6 μL aliquot of the compounds in DMSO was added to the CypA solution in the assay buffer. After being preincubated for 1 h at 4 °C, the assay was started by the addition of chymotrypsin and the substrate. To calculate the half-maximal inhibitory concentration (IC₅₀), a percent of the remaining PPIase activity was plotted against the common logarithm of the compound concentration, and the data were fitted using the sigmoidal fitting model of Origin 7.0 software.

Results

Active Compounds Identification and Synthesis. The 14 chemical structures of CypA inhibitors discovered previously and their interaction fashions to CypA¹⁴ indicate that molecules in the focused library should contain three parts: part A is a relatively hydrophilic head interacting with site A of CypA, part B is hydrophobically interacting with site B, and part L is a linker between A and B, interacting with the “saddle” pocket between sites A and B (Figure 1). According to the structural diversity of the previously discovered binders (or inhibitors), we selected 5 fragments for part A, 17 fragments for part B and 3 linkers for part L. Combining these fragments together, a 5 × 3 × 17 focused

Table 1. Chemical Structures, Docking Binding Energies, SPR Binding Affinities, and PPIase Inhibitory Activities of the 16 Compounds Selected from the Focused Library Using Virtual Screening

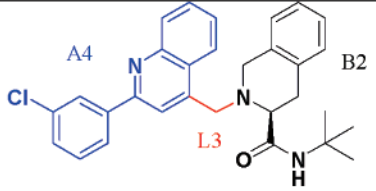
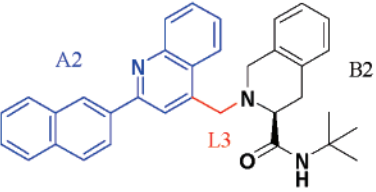
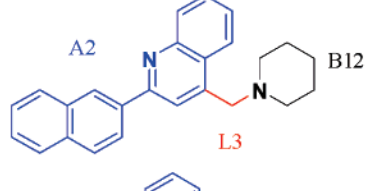
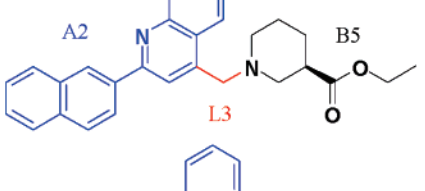
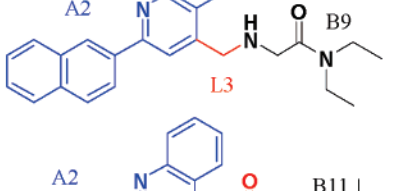
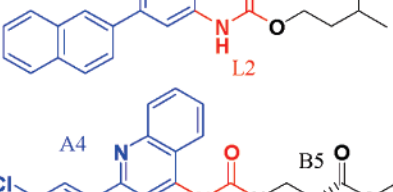
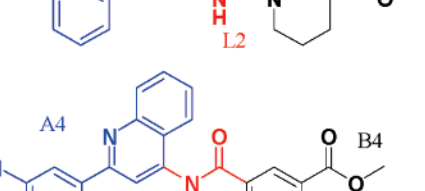
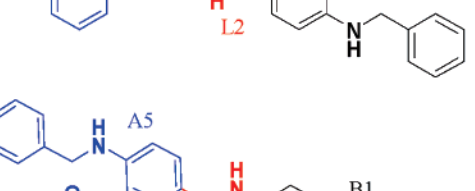
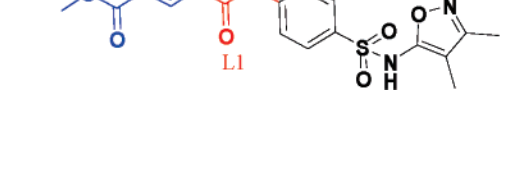
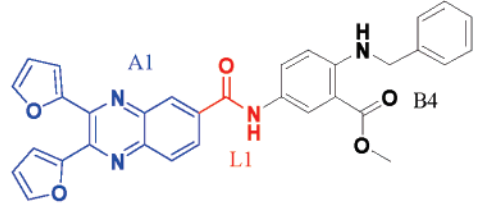
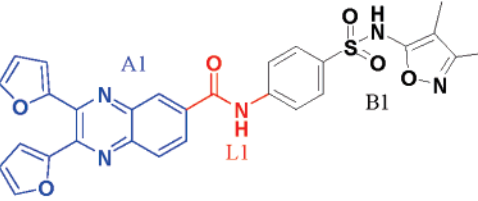
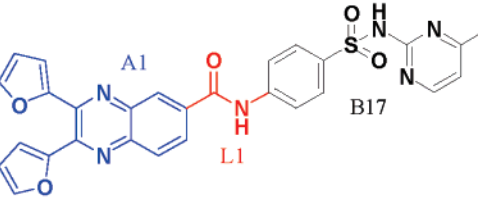
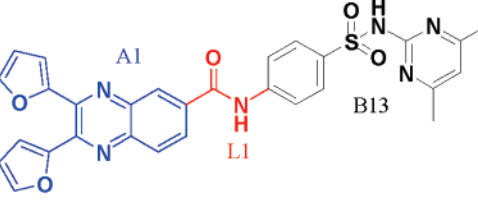
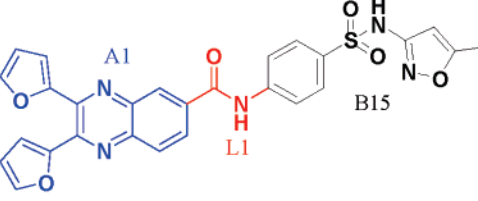
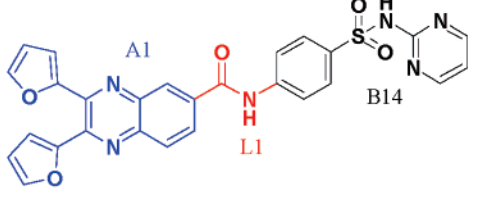
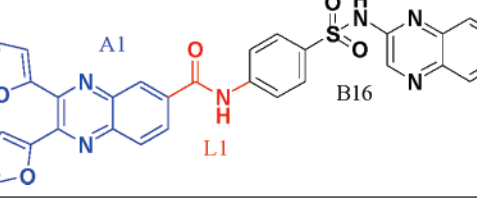
Compound	Structure	BE ₁ ^a	BE ₂ ^b	K _D ^c (μM)	% inhibition at 10 μM / IC ₅₀ (μM) ^d
1a		-33.01	-8.77	24.3	Inactive
1b		-33.77	-8.03	3.07	3
1c		-31.54	-7.57	0.212	2
1d		-34.32	-6.73	17.2	27
1e		-45.51	-6.08	3.41	40
2a		-33.97	-7.67	0.0762	17
2b		-36.23	-7.54	28.8	10
3a		-44.59	-7.26	8.18	35
3b		-43.58	-8.12	10.8	12

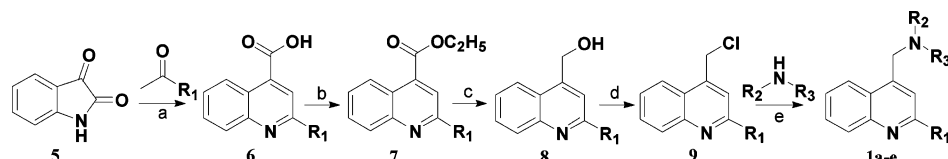
Table 1 (Continued)

Compound	Structure	BE ₁ ^a	BE ₂ ^b	K _D ^c (μM)	% inhibition at 10 μM / IC ₅₀ (μM) ^d
4a		-50.62	-9.29	8.19	91 / 0.25
4b		-47.42	-7.44	27.3	35
4c		-50.38	-9.01	41.0	68 / 6.43
4d		-51.08	-9.27	30.8	22
4e		-51.86	-10.91	38.7	69/2.86
4f		-49.47	-10.84	22.8	80 / 0.96
4g		-52.88	-10.88	35.3	87 / 0.78

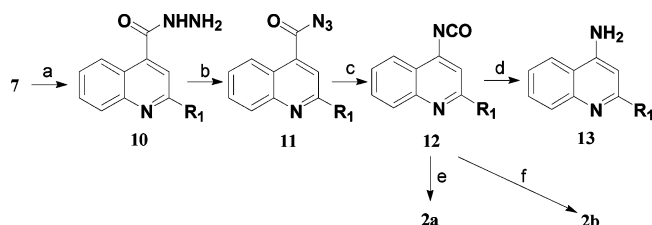
^a The binding energy (BE₁) calculated using DOCK. ^b The binding energy (BE₂) calculated using AutoDock. ^c Data obtained from SPR-based binding affinity assay. K_D represents the dissociation constant. ^d Data are means of three independent experiments.

library was obtained by using LD1.0.¹⁵ Targeting the crystal structure of CypA,¹² the focused library was screened by using the scoring function of DOCK4.0^{18,19} that has been encoded in LD1.0. The interaction energies of these 255 molecules to CypA calculated by DOCK4.0 function range from -52.88 to -27.51 kcal/mol. However, docking pro-

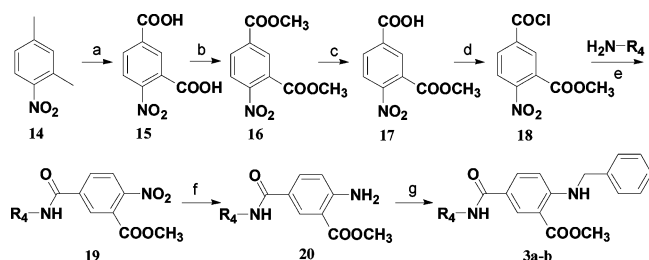
grams and scoring functions have a tendency to generate a significant number of false positives.³¹ Accordingly, to reduce the number of false positives in compound selection, the interaction energies of these 255 molecules with CypA were reevaluated using the AutoDock scoring function,²⁰ which shows a better ability to predict the binding energy.³²

Scheme 1^a

^a Reagents and conditions: (a) (i) KOH, C₂H₅OH, H₂O, reflux; (ii) HCl, H₂O; (b) C₂H₅OH, conc H₂SO₄, reflux; (c) AlLiH₄, THF, 25 °C; (d) SOCl₂, reflux; (e) NMP, Na₂CO₃, 90 °C.

Scheme 2^a

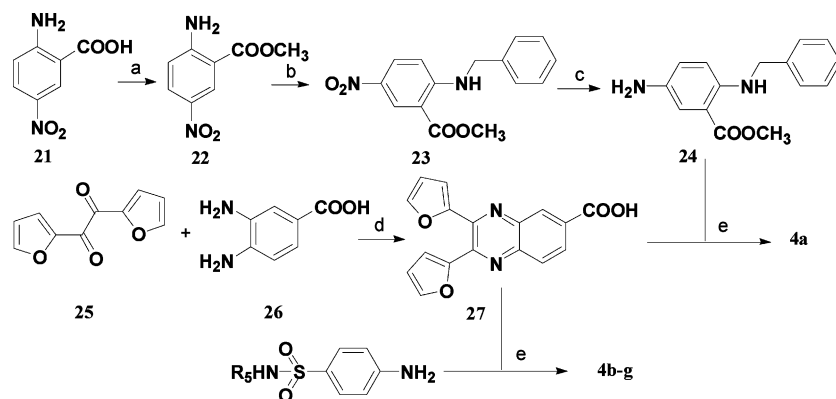
^a Reagents and conditions: (a) N₂H₄·H₂O (85%), C₂H₅OH, reflux; (b) NaNO₂ (1 M), HCl (1 M); (c) toluene, reflux; (d) NaOH, CH₃OH, reflux; (e) isoamyl alcohol, toluene, reflux; (f) (*R*)-(-)-ethyl nipecotate,²⁰ toluene, reflux.

Scheme 3^a

^a Reagents and conditions: (a) (i) KMnO₄, H₂O, reflux; (ii) conc HCl; (b) CH₃OH, conc H₂SO₄, reflux; (c) (i) NaOH (1.2 equiv), CH₃OH; (ii) conc HCl; (d) SOCl₂, reflux; (e) pyridine, CH₂Cl₂; (f) (i) Sn, conc HCl, C₂H₅OH, reflux; (ii) NaHCO₃; (g) benzyl bromide, NMP, Na₂CO₃.

AutoDock calculation indicates that the binding free energies of the compounds to CypA range from -10.91 to -2.90 kcal/mol. Considering these two scoring results, structural diversity, and synthetic feasibility, 16 compounds (**1a-e**, **2a,b**, **3a,b**, and **4a-g**) were selected and synthesized for actual biological testing, and their chemical structures and binding affinities from different scoring functions are listed in Table 1.

These 16 compounds were synthesized through the routes outlined in Schemes 1-4, and the details for synthetic

Scheme 4^a

^a Reagents and conditions: (a) CH₃OH, conc H₂SO₄, reflux; (b) benzyl bromide, NMP, Na₂CO₃; (c) (i) Sn, conc HCl, C₂H₅OH, reflux, (ii) NaHCO₃; (d) C₂H₅OH, reflux; (e) (i) SOCl₂, CH₂Cl₂, reflux; (ii) pyridine, CH₂Cl₂.

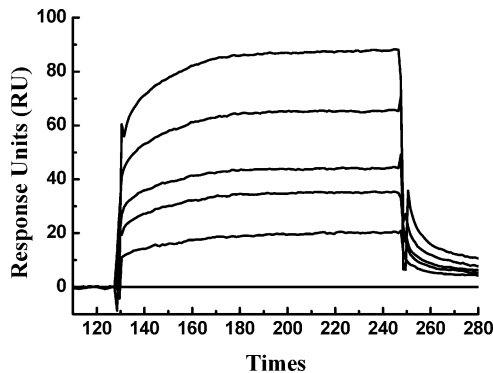


Figure 2. Sensorgram for compound **4a** binding to CypA surface on the CM5 sensor chip. Binding responses are shown for **4a** injected at concentrations of 0, 2.4, 3.4, 4.9, 7, and 10 μM (from bottom to top).

procedures and structural characterizations are described in the Experimentals Section.

Biological Activities. 1. Binding Affinities of the Synthesized Compounds to CypA. Because enzymatic assay is time-consuming, surface plasmon resonance (SPR) measurements were used for the primary screening to determine the binding affinity of these 16 candidate molecules to CypA. The biosensor RUs of the 16 compounds were concentration-dependent, and the collected data indicated these 16 compounds can bind to CypA *in vitro*. Their binding affinities to CypA are in the micromolar range ($K_D = 0.076$ – 41.0 μM). These compounds could be designated as binders (or hits) of CypA. Their binding affinities are shown in Table 1, and a sensorgram for compound **4a**, as an example, is shown in Figure 2.

2. The PPIase Activity of CypA. For the primary assay, the percent inhibitions of the compounds at 10 μM were measured. The results are listed in Table 1. The PPIase activities of compounds **1-4** do not consistently correlate

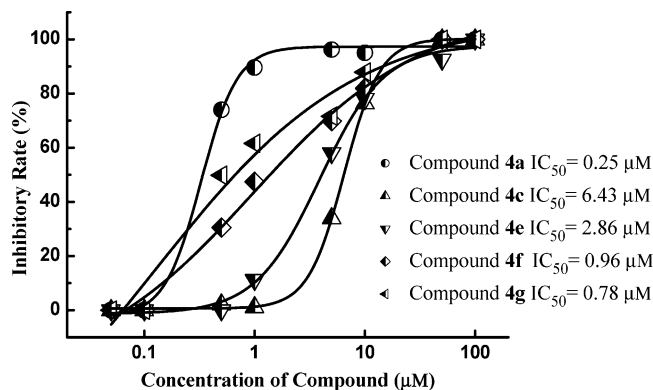


Figure 3. Concentration dependence of PPIase activity by compounds **4a**, **4c**, and **4e–g**. The concentration of CypA was kept constant at 25 nM while the concentration of the compounds ranged from 0.05 to 200 μM .

with the SPR binding affinities as our previously published inhibitors.¹⁴ The reason may be that the protein was immobilized to a sensor chip in the SPR assay, which affects the conformational flexibility of the protein. Accordingly, good binders identified by SPR assay may not be good inhibitors. Five compounds, i.e., **4a**, **4c**, and **4e–g**, can remarkably inhibit the PPIase activity of CypA (percent inhibition at 10 μM >50%), indicating that these five compounds are CypA inhibitors. Therefore, we determined their IC_{50} values, which are, respectively, 0.25, 6.43, 2.86, 0.96, and 0.78 μM (Table 1). The graph of percent inhibition versus concentration of **4a**, **4c**, and **4e–g** is shown in Figure 3.

Discussion

Effectiveness of the Approach. The new approach for focused library design, LD1.0,¹⁵ which integrates special descriptor sets for molecular diversity, druglikeness and molecular docking, has been used to discover new chemical entities of CypA inhibitors. The effectiveness of this approach could be reflected by the hit rate (defined as the number of compounds that bind at a particular concentration divided by the number of compounds experimentally tested). On the basis of the chemical structures of the active compounds discovered previously¹⁴ and their binding models to CypA, we designed a small library containing only 255 compounds. From the library, 16 compounds were selected through docking screening and drug-like analysis for further synthesis and bioassay. All of these 16 compounds are binders of CypA (Table 1). Accordingly, the hit rate of our design and screening approach is $\sim 100\%$ regarding to binding. Of the 16 binders, 5 compounds showed high potent PPIase activities (Table 1 and Figure 3), indicating that the hit rate with the enzymatic inhibitory activity under micromolar levels is as high as $\sim 31.25\%$. Remarkably, the IC_{50} values of our new designed CypA inhibitors (0.25–6.43 μM , Table 1 and Figure 3) in this study are moderately improved, ~ 2 times in comparison with our previously discovered inhibitors (2.5–6.2 μM),¹⁴ and the activity of the most potent one (0.25 μM) increased ~ 10 times. This demonstrates that our approach can not only enrich the hit rate of active compounds but also increase the inhibitory potency of the enzyme inhibitors. Therefore, we might conclude that our

approach, focused library design method LD1.0 including drug-like analysis and virtual screening combined with chemical synthesis and bioassay, is effective in discovering active compounds against the 3D structure of a target.

Structure Activity Relationship Correcting with the Binding Models. Bioassay indicates that, of the 16 binders, 5 compounds show PPIase activity. Structurally, all 5 potent CypA inhibitors contain the A1 fragment (Figure 1), indicating that A1 is the most optimized fragment for part A. L1 is the most favorable fragment for the linker between parts A and B. For part B, fragments that can be adopted by the inhibitors are relatively diverse; fragments B4 and B14–B17 are the building blocks of part B for the CypA inhibitors. Accordingly, as the CypA inhibitors, the building blocks for parts A and L are fixed at fragments A1 and L1, and the fragment for part B is a little bit flexible.

To address the structure–activity relationship and reveal the reason the CypA inhibitors (**4a**, **4c**, and **4e–g**) selected the fragments as their building blocks to compose these inhibitors, we isolated the structures of the inhibitor–CypA complexes from the docking simulation. The result is shown in Figure 4. The 3D structure of CypA itself indicates that the binding groove of CypA consists of two sites: Site A is a small binding pocket formed by Lys82, Met100, Ala101, Asn102, Ala103, Thr107, Asn108, Gly109, Ser110, Gln111, and Phe112. Near to site A, there is a larger pocket, which is called site B, formed by Phe60, Met61, Gln63, Ala101, Asn102, Ala103, Phe113, Leu122, and His126. There is a “saddle” between the two sites (Figure 4a). For the CypA binders and inhibitors, part A fits into site A, part B is located in site B, and part L interacts with the saddle pocket (Figure 4a). Because site B is larger than site A, fragments for part B are structurally more diverse than fragments for part A. In addition, of the five fragments for part A, the shape complementarity between A1 and site A is the most favorable; and one quinoxaline–NH group forms a hydrogen bond with the carbonyl group of Thr73. Thus, all five CypA inhibitors used A1 as a building block for part A. Fragment L1 is a carboxamido group, linking fragment A with its carbonyl C atom and fragment B with its amide N atom. In this way, the amide N atom of L1 forms a hydrogen bond with the backbone carbonyl group of Asn102, and the carbonyl O atom of L1 hydrogen bonds to the amide N atom of Gln63. This carboxamide linker acting as an anchor fixes the binding orientations of the inhibitors to CypA. Interestingly, fragment L2 is also a carboxamido-group; however, it links fragments A and B with an appositive orientation of L1 (Figure 1) so that L2 cannot form hydrogen bonds to Gln63 and Asn120. This is the reason the active inhibitors did not select L2 as their linker. L3 is just a methylene group, which is not able to form a hydrogen bond with CypA. Thus, compounds containing L3 have no PPIase activity. Two kinds fragments were selected as the optimized building blocks for part B, namely, B4 and B14–B17 containing a sulfonamide group. Taking B4 as a building block of part B produced the most potent CypA inhibitor, **4a**, with an IC_{50} of 0.25 μM . Figure 4b shows the interaction model of **4a** to CypA. In addition to the interactions of A1 and L1 to CypA, **4a** has an additional interaction with site B through fragment

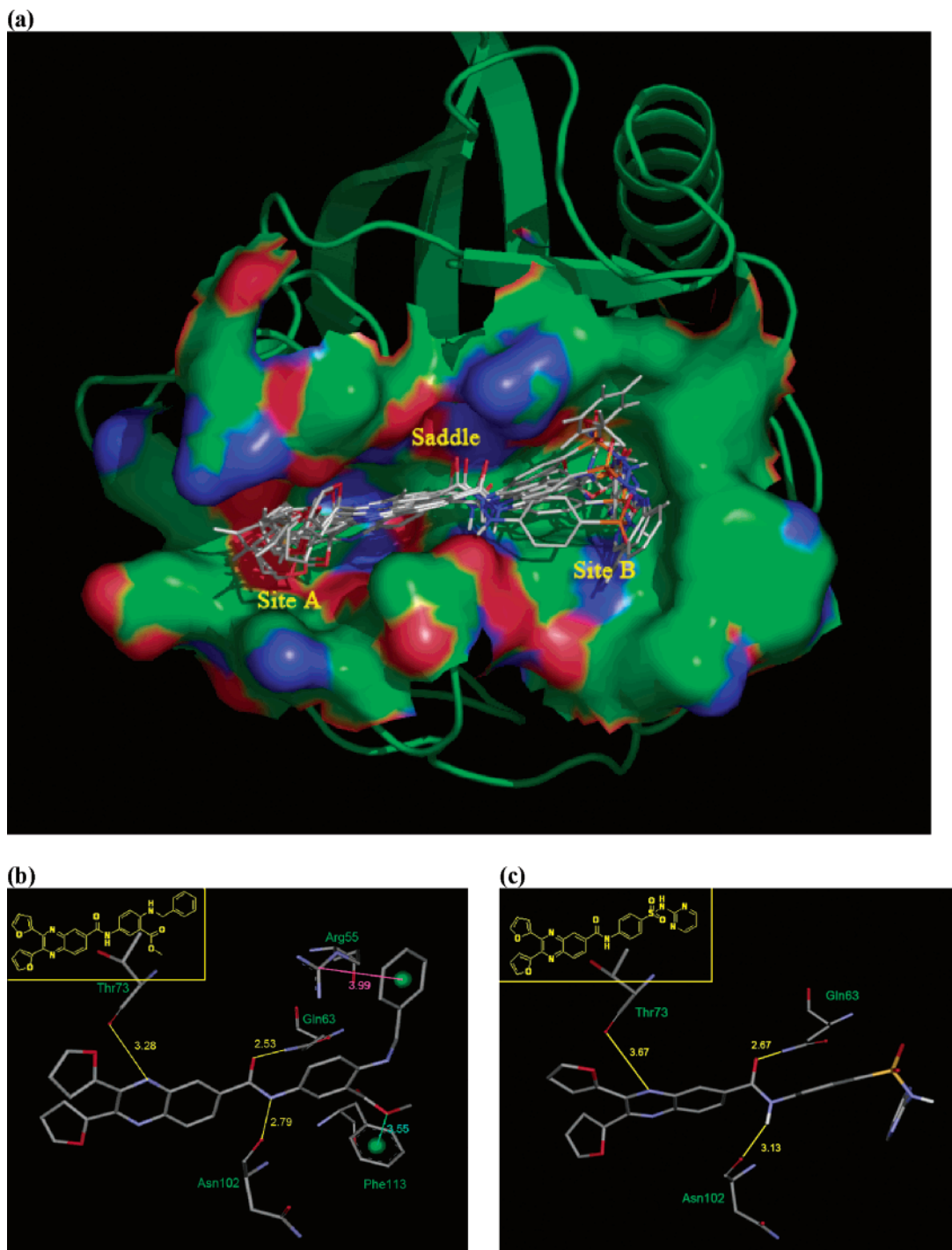


Figure 4. (a) Three-dimensional structural modes of CypA inhibitors (**4a**, **c**, and **e–g**) to CypA derived from the docking simulations. The CypA surface was colored by electrostatic potential. This image was generated using the PyMol program (<http://www.pymol.org/>). (b)–(c) Detailed interactions of **4a** and **4f** with the binding sites of CypA. Hydrogen bonds are represented by yellow lines, cation- π interaction is dictated by pink lines, and p- π interaction is designated by a cyan line. These pictures were prepared using ViewerPro (<http://www.accelrys.com/>).

B4. For example, the guanidine cation of Arg55 has an a cation- π interaction³³ with the benzene ring of B4, and the ester O atom of B4 binds to the benzene ring of Phe113 through p- π interaction.^{34,35} Taking fragments B14–17 as building blocks of part B produced the CypA inhibitors **4c** and **4e–g**. Figure 4c shows the interaction model of these inhibitors to CypA taking **4f** as an example. Figure 4c indicates that interactions of A1 and L1 of the second kind of inhibitors to CypA are reserved, but interaction to site B

through fragments B14–B17 is not visible. This explains why the inhibitory activity of **4a** is higher than that of **4c** and **4e–g**.

Conclusions

The discovery of CypA inhibitors is now of special interest in the treatment of immunological disorders.^{36,37} In the present study, on the basis of the chemical structures of the CypA binders and inhibitors we discovered previously¹⁴ and

their models of interaction to the enzyme, a $5 \times 3 \times 17$ focused library has been designed by using the combinatorial library design program LD1.0.¹⁵ The effectiveness of LD1.0 was demonstrated by the hit rate for discovering CypA binders and inhibitors. Through virtual screening and druglike analysis, 16 compounds were selected from the focused library for chemical synthesis and bioassay. All 16 compounds are CypA binders with dissociation constants (K_D values) ranging from 0.076 to 41.0 μM . Remarkably, 5 compounds (**4a**, **4c**, and **4e–g**) among the 16 binders show PPIase inhibitory activities, with IC_{50} values ranging from 0.25 to 6.43 μM (Table 1). The hit rates for binders and inhibitors are 100 and 31.25%, respectively. In comparison with our previous results,¹⁴ both the binding affinities and inhibitory activities of the active compounds designed in this cycle are moderately improved (Table 1). The five most potent CypA inhibitors were ranked as the top candidates by virtual screening, indicating that the virtual screening strategy encoded in LD1.0 is practical. Docking simulations demonstrated that all five of the best inhibitors (**4a**, **4c**, and **4e–g**) bind to the binding pocket of CypA in a similar way: part A fits into site A, part B is located in site B, and part L interacts with the saddle site of CypA. The bioassay results indicate that the fragment combinations for potent CypA inhibitors are A1 and L1 in conjunction with B4 and B14–17. In addition, all the active compounds discovered in this study are new chemical entities with broad diversity, so they may be good lead compounds for discovering new therapies against the CypA pathway.

Experimental Section

The reagents (chemicals) were purchased from Shanghai Chemical Reagent Company (Lancaster and Acros) and were used without further purification. The type of analytical thin-layer chromatography (TLC) was HSGF 254 (0.15–0.2 mm thickness, Yantai Huiyou Company, China). Yields were not optimized. Melting points were measured in a capillary tube on a SGW X-4 melting point apparatus without correction. Nuclear magnetic resonance (NMR) spectra were obtained on a Bruker AMX-400 NMR (TMS as IS). Chemical shifts are reported in parts per million (ppm, δ) downfield from tetramethylsilane. Proton coupling patterns are described as singlet (s), doublet (d), triplet (t), quartet (q), multiplet (m), and broad (br). Low- and high-resolution mass spectra (LRMS and HRMS) were obtained with electric and electrospray (EI and ESI) from a Finnigan MAT-95 and an LCQ-DECA spectrometer.

Ethyl 2-(3-Chlorophenyl)-quinoline-4-carboxylate 7a. Isatin **5** (17.0 mmol), 3-chloroacetophenone (20.4 mmol), and 85% KOH pellets (51 mmol) were dissolved in EtOH (40 mL), and the reaction mixture was stirred at 80 °C for 24 h. The mixture was condensed, diluted with water, and acidified with conc HCl; and the precipitate was collected, washed, and dried to afford **6a** (3.8 g). Yield 80%; mp 216–218 °C (lit.²⁴ 215–216 °C); EI-MS m/z 282 ($\text{M}^+ - 1$), 238 (100%).

A mixture of **6a** (1 g, 0.55 mmol) and conc H_2SO_4 (0.5 mL) in ethanol (30 mL) was refluxed for 5 h, and most of

the solvent was evaporated, filtered, washed, and dried to afford **7a** (0.75 g, 68%) as a pale yellow solid. mp 108–109 °C. $^1\text{H NMR}$ (CDCl_3): δ 1.56 (t, 2H), 4.62 (q, 3H), 7.50 (m, 2H), 7.70 (t, 1H), 7.84 (t, 1H), 8.11 (m, 1H), 8.27 (m, 2H), 8.37 (s, 1H), 8.78 (d, 1H).

2-(3-Chlorophenyl)-4-chloromethyl-quinoline 9a. A solution of **7a** (0.5 g, 1.6 mmol) in THF (5 mL) was added dropwise to a room-temperature suspension of AlLiH_4 (0.1 g, 2.6 mmol) in THF (5 mL). After 1 h, the reaction was carefully quenched with 0.2 mL of H_2O , 0.2 mL of 15% aqueous NaOH, and an additional 0.6 mL of H_2O . The mixture was stirred for 1 h, filtered, and washed. The filtrate was concentrated, and the precipitated solids were collected to give **8a** (0.29 g). Yield 67%; mp 93–95 °C. $^1\text{H NMR}$ (CDCl_3): δ 5.27 (s, 2H), 7.45 (m, 2H), 7.60 (t, 1H), 7.80 (t, 1H), 7.97 (m, 2H), 8.06 (m, 1H), 8.18 (s, 1H), 8.25 (d, 1H).

A suspension of **8a** (0.25 g, mmol) in redistilled SOCl_2 (6 mL) was refluxed gently for 3 h. A clear solution resulted. The SOCl_2 was then evaporated under reduced pressure. The yellow solid **9a** (130 mg, 50%) thus obtained was used in the next step without further purification. EI-MS m/z 287 (M^+ , 100%).

(S)-(–)-N-tert-Butyl-2-[2-(3-chlorophenyl)-quinolin-4-ylmethyl]-1,2,3,4-tetrahydro-3-isoquinolinecarboxamide 1a. To a stirred mixture of **9a** (100 mg, 0.35 mmol), NaCO_3 (80 mg, 0.75 mmol), and *N*-methyl-2-pyrrolidone (NMP) (3 mL) was added *(S)-(–)-N-tert-butyl-1,2,3,4-tetrahydro-3-isoquinolinecarboxamide* (82 mg, 0.35 mmol). The mixture was then heated at 90 °C for 10 h. The reaction mixture after cooling was transferred to a separatory funnel using a 1:1 mixture of H_2O and EtOAc. The product was extracted with EtOAc. The combined organic phases were washed, dried, filtered, and concentrated. The residue was purified by flash column chromatography on silica gel and eluted with a mixture of EtOAc/petroleum ether (1:20, v/v) to afford **1a** (100 mg) as a white solid. Yield 60%; mp 65–67 °C; $[\alpha]_{\text{D}}^{20} = -19.1^\circ$ ($c = 0.305$ in CH_2Cl_2). $^1\text{H NMR}$ (CDCl_3): δ 1.04 (s, 9H), 3.21 (d, 2H), 3.59 (t, 1H), 3.97 (q, 4H), 4.25 (q, 4H), 6.88 (s, 1H), 7.06 (d, 1H), 7.26 (m, 2H), 7.50 (m, 2H), 7.60 (t, 1H), 7.80 (t, 1H), 7.85 (s, 1H), 8.10 (m, 2H), 8.24 (m, 2H); EI-MS m/z 483 (M^+), 383 (100%). HRMS (EI) m/z calcd $\text{C}_{30}\text{H}_{30}\text{ClN}_3\text{O}$ (M^+) 483.2059, found 483.2078.

2-Naphthalen-2-yl-4-chloromethylquinoline 9b. In the same manner as described for **9a**, **9b** was prepared from 2-acetonaphthone; mp 143–145 °C; EI-MS m/z 303 (M^+ , 100%).

(S)-(–)-N-tert-Butyl-2-(2-naphthalen-2-ylquinolin-4-ylmethyl)-1,2,3,4-tetrahydro-3-isoquinolinecarboxamide 1b. In the same manner as described for **1a**, **1b** was prepared from **9b** and *(S)-(–)-N-tert-butyl-1,2,3,4-tetrahydro-3-isoquinolinecarboxamid*. Yield 68%; mp 64–66 °C; $[\alpha]_{\text{D}}^{20} = -17.0^\circ$ ($c = 0.295$ in CH_2Cl_2). $^1\text{H NMR}$ (CDCl_3): δ 1.08 (s, 9H), 3.23 (d, 2H), 3.62 (t, 1H), 4.00 (q, 4H), 4.25 (q, 4H), 6.98 (s, 1H), 7.07 (d, 1H), 7.28 (m, 2H), 7.61 (m, 3H), 7.81 (t, 1H), 7.93 (m, 1H), 8.10 (m, 4H), 8.39 (m, 2H), 8.64 (s, 1H); ESI-MS m/z 500 [$\text{M} + \text{H}$]⁺. HRMS (ESI) m/z calcd $\text{C}_{34}\text{H}_{34}\text{N}_3\text{O}$ [$\text{M} + \text{H}$]⁺ 500.2702, found 500.2697.

2-Naphthalen-2-yl-4-piperidin-1-ylmethylquinoline 1c. In the same manner as described for **1a**, **1c** was prepared

from **9b** and piperidine. Yield 28%; mp 69–71 °C. ¹H NMR (CDCl₃): δ 1.53 (m, 2H), 1.69 (m, 4H), 2.56 (m, 4H), 4.00 (s, 2H), 7.57 (m, 3H), 7.76 (t, 1H), 7.91 (m, 1H), 8.02 (m, 2H), 8.11 (s, 1H), 8.27 (t, 2H), 8.41 (d, 1H), 8.65 (s, 1H); EI-MS *m/z* 352 (M⁺), 269 (100%). HRMS (EI) *m/z* calcd C₂₅H₂₄N₂ (M⁺) 352.1939, found 352.1939.

(R)-(–)-Ethyl 1-(2-Naphthalen-2-ylquinolin-4-ylmethyl)-piperidine-3-carboxylate 1d. (±)-Ethyl nipecotate (4.91 g, 31 mmol) and L-(+)-tartaric acid (4.68 g, 31 mmol) were dissolved in a hot mixture solvent (ethanol, 25 mL; acetone, 7 mL) and slowly cooled to room temperature (r.t.) (R)-(–)-Ethyl nipecotate (0.92 g) was gained as a pale yellow oil.²⁶ [α]_D²⁰ = –0.80° (*c* = 2.31 in CHCl₃) (lit.²⁶ [α]_D²⁵ = –0.95° (*c* = 1.2 in CHCl₃)).

In the same manner as described for **1a**, **1d** was prepared from **9b** and (R)-(–)-ethyl nipecotate. Yield 54%; mp 33–35 °C; [α]_D²⁰ = –4.6° (*c* = 0.325 in CHCl₃). ¹H NMR (CDCl₃): δ 1.25 (t, 3H), 1.60 (m, 3H), 1.93 (m, 1H), 2.31 (m, 1H), 2.63 (m, 2H), 2.79 (m, 1H), 2.99 (m, 1H), 4.13 (m, 4H), 7.55 (m, 3H), 7.77 (t, 1H), 7.92 (m, 1H), 8.07 (m, 3H), 8.26 (d, 2H), 8.41 (d, 1H), 8.66 (s, 1H); EI-MS *m/z* 424 (M⁺), 269 (100%). HRMS (EI) *m/z* calcd C₂₈H₂₈N₂O₂ (M⁺) 424.2157, found 424.2151.

***N,N*-Diethyl-2-[(2-naphthalen-2-yl-quinolin-4-ylmethyl)-amino]-acetamide 1e.** In the same manner as described for **1a**, **1e** was prepared from **9b** and 2-amino-*N,N*-diethylacetamide. Yield 30%; mp 68–70 °C. ¹H NMR (CDCl₃): δ 1.11 (3H, t), 1.21 (3H, t), 3.33 (2H, q), 3.40 (2H, q), 4.22 (2H, d), 4.27 (br, 1H), 5.14 (s, 2H), 7.53 (m, 3H), 7.79 (t, 1H), 7.92 (m, 1H), 8.08 (m, 3H), 8.26 (d, 2H), 8.42 (d, 1H), 8.70 (s, 1H); EI-MS *m/z* 397 (M⁺). HRMS (EI) *m/z* calcd C₂₆H₂₇N₃O (M⁺) 397.2150, found 397.2154.

2-(3-Chlorophenyl)-4-isocyanato-quinoline 12a. A mixture of **7a** (1 g, 3.2 mmol) and N₂H₄·H₂O (0.5 mL) in ethanol (30 mL) was refluxed for 8 h, and most of the solvent was evaporated, filtered, washed, and dried to afford **10a** (0.75 g, 79%) as a pale yellow solid. mp 204–205 °C.

To a stirred solution of **10a** (0.94 g, 3.16 mmol) in hydrochloric acid (2 N, 8 mL) was added a –3 °C solution of NaNO₂ (0.55 g, 7.9 mmol) in H₂O (8 mL). After 2 h, the precipitated solids were collected to give **11a** (0.89 g). Yield 92%; mp 106–108 °C.

A solution of **11a** (0.89 g) in toluene (16 mL) was refluxed for 8 h and then cooled to r.t., and the precipitated solids were collected to give **12a** (0.5 g). Yield 62%; mp 280–282 °C; EI-MS *m/z* 280 (M⁺, 100%).

2-Naphthalen-2-yl-4-isocyanatoquinoline 12b. In the same manner as described for **12a**, **12b** was prepared as a yellow solid. Yield 50%; mp >300 °C; EI-MS *m/z* 296 (M⁺, 100%).

2-(3-Chlorophenyl)-quinolin-4-ylamine 13a. A mixture of **12a** (100 mg, 0.36 mmol) and NaOH (100 mg) in methanol (30 mL) was refluxed for 24 h. The mixture was condensed, and the residue was purified by flash column chromatography on silica gel and eluted with a mixture of CH₃OH/CH₂Cl₂ (1:10, v/v) to afford **13a** (52 mg) as a pale yellow solid. Yield 57%; mp 139–141 °C. ¹H NMR (CDCl₃): δ 4.78 (br, 2H), 7.04 (s, 1H), 7.50 (m, 3H), 7.72 (t, 1H), 7.78 (d, 1H), 7.97 (m, 1H), 8.10 (m, 2H)

(R)-(–)-Ethyl 1-[2-(3-Chlorophenyl)-quinolin-4-ylcarbamoyl]-piperidine-3-carboxylate 2a. A mixture of **12a** (100 mg, 0.36 mmol) and (R)-(–)-ethyl nipecotate (57 mg, 0.36 mmol) in toluene (10 mL) was refluxed for 48 h. The mixture was condensed, and the residue was purified by flash column chromatography on silica gel and eluted with a mixture of EtOAc/petroleum ether (1:10, v/v) to afford **2a** (55 mg) as a white solid. Yield 35%; [α]_D²⁰ = –87.3° (*c* = 0.55 in CHCl₃). ¹H NMR (CDCl₃): δ 1.38 (t, 3H), 1.50 (m, 1H), 1.80 (m, 1H), 1.94 (m, 1H), 2.15 (m, 1H), 2.41 (m, 1H), 2.92 (m, 2H), 3.48 (m, 1H), 4.36 (m, 3H), 7.54 (m, 2H), 7.70 (m, 1H), 7.88 (d, 1H), 8.05 (m, 1H), 8.44 (m, 3H), 9.30 (s, 1H); EI-MS *m/z* 437 (M⁺), 280 (100%). HRMS (EI) *m/z* calcd C₂₄H₂₄ClN₃O₃ (M⁺) 437.1506, found 437.1506.

(2-Naphthalen-2-ylquinolin-4-yl)-carbamic Acid 3-Methyl Butyl Ester 2b. A mixture of **12b** in the same manner as described for **2a** and **2b** was prepared from **12b** and isoamyl alcohol. Yield 45%; mp 143–145 °C. ¹H NMR (CDCl₃): δ 1.03 (d, 6H), 1.73 (q, 2H), 1.85 (m, 1H), 4.39 (t, 2H), 7.61 (m, 3H), 7.85 (m, 2H), 7.93 (m, 1H), 8.05 (m, 2H), 8.42 (m, 2H), 8.70 (s, 1H), 8.86 (s, 1H); EI-MS *m/z* 384 (M⁺), 270 (100%). HRMS (EI) *m/z* calcd C₂₅H₂₄N₂O₂ (M⁺) 384.1848, found 384.1838.

4-Nitroisophthalic Acid 3-Methyl Ester 17. This compound was prepared by the method of Axer²⁸ from 4-nitroisophthalic acid **15**.²⁷ mp 186–188 °C (lit.²⁸ 192–194 °C). ¹H NMR (CDCl₃): δ 3.99 (s, 3H), 7.99 (d, 1H), 8.40 (dd, 1H), 8.54 (d, 1H).

6-Amino-*N*-[2-(3-chlorophenyl)-quinolin-4-yl]-isophthalamic Acid Methyl Ester 20a. The preparation of *N*-[2-(3-chlorophenyl)-quinolin-4-yl]-6-nitro-isophthalamic acid methyl ester **19a** was performed according to our previously reported procedures.¹⁴ A mixture of **19a** (40 mg, 0.09 mmol), Sn (40 mg), and conc HCl (0.5 mL) in ethanol (10 mL) was refluxed for 2 h, and the mixture was filtered, concentrated, and cooled to r.t., and the precipitated solids were collected to give **20a** (30 mg, 80%) as a pale yellow solid. ¹H NMR (CDCl₃): δ 3.99 (s, 3H), 5.02 (br, 2H), 7.45 (t, 2H), 7.61 (t, 1H), 7.81 (t, 1H), 7.88 (d, 1H), 8.05 (m, 2H), 8.27 (m, 3H), 8.35 (s, 1H), 8.76 (s, 1H).

6-Benzylamino-*N*-[2-(3-chlorophenyl)-quinolin-4-yl]-isophthalamic Acid Methyl Ester 3a. In the same manner as described for **1a**, **3a** was prepared from **20a** and benzyl bromide. Yield 55%; mp 39–40 °C. ¹H NMR (CDCl₃): δ 3.58 (s, 3H), 1.50 (m, 1H), 5.03 (s, 2H), 6.38 (m, 2H), 7.15 (m, 5H), 7.42 (m, 3H), 7.65 (m, 2H), 7.80 (m, 2H), 7.96 (m, 2H), 8.45 (s, 1H); EI-MS *m/z* 521 (M⁺), 178 (100%). HRMS (EI) *m/z* calcd C₃₁H₂₄ClN₃O₃ (M⁺) 521.1528, found 521.1506.

***N*-(3,4-Dimethylisoxazol-5-yl)-4-[(3-methoxycarbonyl)-4-benzylamino]-benzamido]-benzenesulfonamide 3b.** In the same manner as described for **3a**, **3b** was prepared from **18** and sulfisoxazole; mp 84–86 °C. ¹H NMR (CDCl₃): δ 1.68 (s, 3H), 2.12 (s, 3H), 3.91 (s, 3H), 4.59 (s, 2H), 6.77 (d, 1H), 7.27 (m, 5H), 7.79 (d, 2H), 7.87 (d, 2H), 8.12 (d, 1H), 8.41 (d, 1H); EI-MS *m/z* 534 (M⁺), 178 (100%). HRMS (EI) *m/z* calcd C₂₇H₂₆N₄O₆S (M⁺) 534.1590, found 534.1573.

Methyl 5-Amino-2-benzylaminobenzoate 24. In the same manner as described for **16**, methyl 2-amino-5-nitrobenzoate

22 was prepared from **21**. mp 158–160 °C. ¹H NMR (CDCl₃): δ 3.93 (s, 3H), 6.68 (d, 1H), 8.15 (dd, 1H), 8.84 (d, 1H).

A solution of **22** (200 mg, 1.02 mmol), NaCO₃ (200 mg), benzyl bromide (0.26 g 1.53 mmol), and NMP (3 mL) was heated at 90 °C for 48 h. The mixture was condensed, and the residue was purified by flash column chromatography on silica gel and eluted with a mixture of EtOAc/petroleum ether (1:10, v/v) to afford **23** (180 mg) as a yellow solid. Yield 62%. ¹H NMR (CDCl₃): δ 3.93 (s, 3H), 4.56 (d, 2H), 6.67 (d, 1H), 7.38 (m, 5H), 8.18 (dd, 1H), 8.89 (d, 1H).

In the same manner as described for **20**, **24** was prepared from **23**. EI-MS *m/z* 256 (M⁺).

2,3-Difuran-2-yl-quinoxaline-6-carboxylic Acid 27. A solution of furil **25** (1.9 g, 10 mmol) and 3,4-diaminobenzoic acid **26** (1.52 g, 10 mmol) in ethanol (50 mL) was refluxed for 20 h. The mixture was concentrated and cooled to r.t., and the precipitated solids were collected to provide **27** (2.9 g) as a yellow solid. Yield 94%; mp 243–245 °C. ¹H NMR (DMSO): δ 6.77 (d, 2H), 6.86 (dd, 2H), 7.98 (d, 2H), 8.19 (d, 1H), 8.31 (dd, 1H), 8.58 (d, 1H).

Methyl 2-Benzylamino-5-[(2,3-difuran-2-yl)-quinoxaline-6-carboxamido]-benzoate 4a. The preparation of **4a** was performed according to our previously reported procedures.¹⁴ mp 144–146 °C. ¹H NMR (CDCl₃): δ 3.88 (s, 3H), 4.46 (d, 1H), 5.78 (d, 1H), 6.59 (m, 2H), 6.78 (m, 2H), 7.04 (d, 1H), 7.35 (m, 5H), 7.64 (m, 1H), 7.76 (d, 1H), 7.97 (d, 1H), 8.03 (s, 1H), 8.14 (d, 2H), 8.48 (d, 1H); EI-MS *m/z* 544 (M⁺), 289 (100%). HRMS (EI) *m/z* calcd C₃₂H₂₄N₄O₅ (M⁺) 544.1729, found 544.1747.

N-(3,4-Dimethylisoxazol-5-yl)-4-[(2,3-difuran-2-yl)-quinoxaline-6-carboxamido]-benzenesulfonamide 4b. Yield 47%; flash chromatography with EtOAc/petroleum ether (1:2, v/v); mp 256–258 °C. ¹H NMR (DMSO): δ 1.68 (s, 3H), 2.11 (s, 3H), 6.84 (m, 4H), 7.82 (d, 2H), 7.98 (m, 2H), 8.12 (d, 2H), 8.25 (d, 1H), 8.34 (d, 1H), 8.82 (d, 1H); EI-MS *m/z* 555 (M⁺), 289 (100%). HRMS (EI) *m/z* calcd C₂₈H₂₁N₅O₆S (M⁺) 555.1205, found 555.1212.

N-(4-Methylpyrimidin-2-yl)-4-[(2,3-difuran-2-yl)-quinoxaline-6-carboxamido]-benzenesulfonamide 4c. Yield 57%; flash chromatography with EtOAc/petroleum ether (1:2, v/v); mp 246–248 °C. ¹H NMR (DMSO): δ 2.31 (s, 3H), 6.74 (m, 2H), 6.81 (m, 2H), 6.91 (d, 1H), 7.93 (m, 1H), 8.01 (q, 4H), 8.21 (d, 1H), 8.33 (m, 2H), 8.77 (d, 2H); EI-MS *m/z* 552 (M⁺), 289 (100%). HRMS (EI) *m/z* calcd C₂₈H₂₀N₆O₅S (M⁺) 552.1213, found 552.1216.

N-(4,6-Dimethylpyrimidin-2-yl)-4-[(2,3-difuran-2-yl)-quinoxaline-6-carboxamido]-benzenesulfonamide 4d. Yield 63%; flash chromatography with EtOAc/petroleum ether (1:2, v/v); mp 244–246 °C. ¹H NMR (DMSO): δ 2.25 (s, 6H), 6.75 (m, 3H), 6.81 (m, 2H), 7.93 (m, 2H), 8.01 (q, 4H), 8.21 (d, 1H), 8.33 (d, 1H), 8.77 (d, 1H); EI-MS *m/z* 566 (M⁺), 289 (100%). HRMS (EI) *m/z* calcd C₂₉H₂₂N₆O₅S (M⁺) 566.1390, found 566.1372.

N-(5-Methylisoxazol-3-yl)-4-[(2,3-difuran-2-yl)-quinoxaline-6-carboxamido]-benzenesulfonamide 4e. Yield 33%; flash chromatography with EtOAc/petroleum ether (1:2, v/v); mp 275–277 °C. ¹H NMR (DMSO): δ 2.32 (s, 3H), 6.17

(s, 1H), 6.76 (m, 2H), 6.84 (m, 2H), 7.91 (d, 2H), 7.96 (m, 2H), 8.10 (d, 2H), 8.24 (d, 1H), 8.35 (dd, 1H), 8.80 (d, 1H); EI-MS *m/z* 541 (M⁺), 289 (100%). HRMS (EI) *m/z* calcd C₂₇H₁₉N₅O₆S (M⁺) 541.1041, found 541.1056.

N-(Pyrimidin-2-yl)-4-[(2,3-difuran-2-yl)-quinoxaline-6-carboxamido]-benzenesulfonamide 4f. Yield 54%; flash chromatography with EtOAc/petroleum ether (1:2, v/v); mp 290–292 °C. ¹H NMR (DMSO): δ 6.77 (m, 2H), 6.85 (m, 2H), 7.09 (t, 1H), 7.97 (m, 2H), 8.08 (q, 4H), 8.24 (d, 1H), 8.35 (dd, 1H), 8.54 (d, 2H), 8.80 (d, 1H); EI-MS *m/z* 538 (M⁺), 289 (100%). HRMS (EI) *m/z* calcd C₂₇H₁₈N₆O₅S (M⁺) 538.1060, found 538.1059.

N-(Quinoxalin-2-yl)-4-[(2,3-di-furan-2-yl)-quinoxaline-6-carboxamido]-benzenesulfonamide 4g. Yield 24%; flash chromatography with EtOAc/petroleum ether (1:2, v/v); mp 262–263 °C. ¹H NMR (DMSO): δ 6.73 (m, 2H), 6.81 (m, 2H), 7.63 (t, 1H), 7.80 (m, 2H), 7.94 (m, 3H), 8.27 (m, 5H), 8.30 (d, 1H), 8.60 (s, 1H), 8.75 (d, 1H); EI-MS *m/z* 588 (M⁺), 289 (100%). HRMS (EI) *m/z* calcd C₃₁H₂₀N₆O₅S (M⁺) 588.1225, found 588.1216.

Acknowledgment. J.L, J.Z., and J.C. contributed equally to this work. We gratefully acknowledge financial support from the State Key Program of Basic Research of China (Grant 2002CB512802), the National Natural Science Foundation of China (Grants 20372069, 29725203, 20472094, and 20102007), the Basic Research Project for Talent Research Group from the Shanghai Science and Technology Commission, the Key Project from the Shanghai Science and Technology Commission (Grant 02DJ14006), the Key Project for New Drug Research from CAS, the Qi Ming Xing Foundation of Shanghai Ministry of Science and Technology (Grant 03QD14065), and the 863 Hi-Tech Programm (Grants 2002AA233061, 2002AA104270, 2002AA233011, and 2003AA235030).

Note Added after ASAP Publication. This article was released ASAP on April 13, 2006, with an error in a corresponding author's e-mail address and duplicate information in the corresponding author footnotes and Acknowledgments. The version posted on April 21, 2006, and the print version are correct.

References and Notes

- Braaren, D.; Luban, J. *EMBO J.* **2001**, *20*, 1300–1309.
- Handschumacher, R. E.; Harding, M. W.; Rice, J.; Drugge, R. J.; Speicher, D. W. *Science* **1984**, *226*, 544–547.
- Galat, A. *Curr. Top. Med. Chem.* **2003**, *3*, 1315–1347.
- Dornan, J.; Taylor, P.; Walkinshaw, M. D. *Curr. Top. Med. Chem.* **2003**, *3*, 1392–1409.
- Luban, J.; Bossolt, K. L.; Franke, E. K.; Kalpana, G. V.; Goff, S. P. *Cell* **1993**, *73*, 1067–1078.
- Luo, C.; Luo, H. B.; Zheng, S.; Gui, C.; Yue, L.; Yu, C.; Sun, T.; He, P.; Chen, J.; Shen, J.; Luo, X.; Li, Y.; Liu, H.; Bai, D.; Shen, J.; Yang, Y.; Li, F.; Zuo, J.; Hilgenfeld, R.; Pei, G.; Chen, K.; Shen, X.; Jiang, H. *Biochem. Biophys. Res. Commun.* **2004**, *321*, 557–565.
- Chen, Z.; Mi, L.; Xu, J.; Yu, J.; Wang, X.; Jiang, J.; Xing, J.; Shang, P.; Qian, A.; Li, Y.; Shaw, P. X.; Wang, J.; Duan, S.; Ding, J.; Fan, C.; Zhang, Y.; Yang, Y.; Yu, X.; Feng, Q.; Li, B.; Yao, X.; Zhang, Z.; Li, L.; Xue, X.; Zhu, P. *J. Infect. Dis.* **2005**, *191*, 755–760.
- Friedman, J.; Weissman, I. *Cell* **1991**, *66*, 799–806.

- (9) Zou, X. J.; Matsumura, Y. J.; John, P.; Ryo, S.; Alberto, M.; Jack, M.; Stanley, C. J. *Transpl. Immunol.* **1995**, *3*, 151–161.
- (10) Siekierka, J. J.; Hung, S. H.; Poe, M.; Lin, C. S.; Sigal, N. H. *Nature* **1989**, *341*, 755–757.
- (11) Clane, R. Y.; Lim, S.; Samaan, A.; Collier, D. ST.; Pollard, S. G.; White, D. J. G.; Thiru, S. *Lancet* **1989**, *334*, 227.
- (12) Sedrani, R.; Kallen, J.; Martin Cabrejas, L. M.; Papageorgiou, C. D.; Senia, F.; Rohrbach, S.; Wagner, D.; Thai, B.; Jutzi Eme, A.-M.; France, J.; Oberer, L.; Rihs, G.; Zenke, G.; Wagner, J. *J. Am. Chem. Soc.* **2003**, *125*, 3849–3859.
- (13) Li, Q.; Moutiez, M.; Charbonnier, J.-B.; Vaudry, K.; Menez, A.; Quemeneur, E.; Dugave, C. *J. Med. Chem.* **2000**, *43*, 1770–1779.
- (14) Li, J.; Chen, J.; Gui, C.; Zhang, L.; Qin, Y.; Xu, Q.; Zhang, J.; Liu, H.; Shen, X.; Jiang, H. *Bioorg. Med. Chem.* **2006**, *14*, 2209–2224.
- (15) Chen, G.; Zheng, S.; Luo, X.; Shen, J.; Zhu, W.; Liu, H.; Gui, C.; Zhang, J.; Zheng, M.; Puah, C. M.; Chen, K.; Jiang, H. *J. Comb. Chem.* **2005**, *7*, 398–406.
- (16) Zheng, S.; Luo, X.; Chen, G.; Zhu, W.; Shen, J.; Chen, K.; Jiang, H. *J. Chem. Inf. Mod.* **2005**, *45*, 856–862.
- (17) Cui, M.; Huang, X.; Luo, X.; Briggs, J. M.; Ji, R.; Chen, K.; Shen, J.; Jiang, H. *J. Med. Chem.* **2002**, *45*, 5249–5259.
- (18) Ewing, T. J. A.; Kuntz, I. D. *J. Comput. Chem.* **1997**, *18*, 1175–1189.
- (19) Kuntz, I. D. *Science* **1992**, *257*, 1078–1082.
- (20) Morris, G. M.; Goodsell, D. S.; Halliday, R. S.; Huey, R.; Hart, W. E.; Belew, R. K.; Olson, A. J. *J. Comput. Chem.* **1998**, *19*, 1639–1662.
- (21) Weiner, S. J.; Kollman, P. A.; Nguyen, D. T.; Case, D. A. *J. Comput. Chem.* **1986**, *7*, 230–252.
- (22) Gasteiger, J.; Marsili, M. *Tetrahedron* **1980**, *36*, 3219–3228.
- (23) Lipinski, C. A.; Lombardo, F.; Dominy, B. W.; Feeney, P. *J. Adv. Drug Delivery Rev.* **1997**, *23*, 3–25.
- (24) Brown, R. F.; Jacobs, T. L.; Winstein, S.; Kloetzel, M. C.; Spaeth, E. C.; Florsheim, W. H.; Robson, J. H.; Levy, E. F.; Bryan, G. M.; Magnusson, A. B.; Miller, S. J.; Ott, M. L.; Terek, J. H. *J. Am. Chem. Soc.* **1946**, *68*, 2705–2708.
- (25) John, H. *Chem. Ber.* **1926**, *59*, 1447–1452.
- (26) Lee, S.; Im, D.; Cheong, C.; Chung, B. *Heterocycles* **1999**, *51*, 1913–1919.
- (27) Kornblum, N.; Fifolt, M. J. *Tetrahedron* **1989**, *45*, 1311–1322.
- (28) Axer, P. *Monatsh. Chem.* **1920**, *41*, 153–165.
- (29) Helfenbein, J.; Lartigue, C.; Noirault, E.; Azim, E.; Legailiard, J.; Galmier, M. J.; Madelmont, J. C. *J. Med. Chem.* **2002**, *45*, 5806–5808.
- (30) Kofron, J. L.; Kuzmic, P.; Kishore, V.; Colon-Bonilla, E.; Rich, D. H. *Biochemistry* **1991**, *30*, 6127–6134.
- (31) Schneider, G.; Bohm, H. *J. Drug Discovery Today* **2002**, *7*, 64–70.
- (32) Wang, R.; Lu, Y.; Wang, S. *J. Med. Chem.* **2003**, *46*, 2287–2303.
- (33) Dougherty, D. A. *Science* **1996**, *271*, 163–168.
- (34) Gung, B. W.; Xue, X.; Reich, H. J. *J. Org. Chem.* **2005**, *70*, 7232–7237.
- (35) Sarkhel, S.; Rich, A.; Egli, M. *J. Am. Chem. Soc.* **2003**, *125*, 8998–8999.
- (36) Dumont, F. J. *Exp. Opin. Ther. Patents* **2001**, *11*, 377–404.
- (37) Anderson, P. S., Kenyon, G. L., Marshall, G. R. In *Perspectives in Drug Discovery and Design*; ESCOM Science Publishers: Leiden, The Netherlands, 1994; pp 3–248.

CC0501561